



Fluorometric determination of dopamine by using molybdenum disulfide quantum dots

Xinnan Liu¹ · Wentao Zhang¹ · Lunjie Huang¹ · Na Hu² · Wei Liu³ · Yingnan Liu¹ · Sihang Li¹ · Chengyuan Yang¹ · Yourui Suo² · Jianlong Wang¹

Received: 6 January 2018 / Accepted: 12 March 2018 / Published online: 20 March 2018
© Springer-Verlag GmbH Austria, part of Springer Nature 2018

Abstract

A method is described for the rapid fluorometric determination of dopamine (DA) by using molybdenum disulfide quantum dots (MoS₂ QDs) that were fabricated via an ammonium hydroxide etching method. The probe has a fluorescence (with excitation/emission peaks at 267/380 nm) that is quenched by DA with high selectivity over various interferences. This is attributed to a reaction that occurs between DA and the molybdate ions in pH 9 solutions of MoS₂ QDs. The formation of organic molybdate complexes and of dopamine-quinone results in strong quenching of the fluorescence of the QDs which is due to both electron transfer and an inner filter effect. Under the optimum conditions, the assay works in the 0.1–100 μM DA concentration range, with two linear ranges and a 10 nM detection limit. The method was applied to the determination of DA in spiked artificial urine samples, where it gave recoveries ranging from 97.6 to 102.2%, demonstrating that the method a promising tool for rapid and selective detection of DA.

Keywords Dopamine · Dynamic quenching · Etching synthesis · Fluorescent probe · Transition metal dichalcogenides

Introduction

Dopamine (DA) is a crucial catecholamine and neurotransmitter which exists in the renal, hormonal, central nervous system as well as cardiovascular system, playing a significant role in behavioral responses and brain functions [1]. Abnormal DA levels in biological fluids are related to several neural diseases, such as Parkinson's and Alzheimer's

diseases [2]. Therefore, establishing quantitative detection method of DA concentration is crucial for clinical diagnosis of those diseases.

Various approaches have been developed for DA determination such as high performance liquid chromatography [3], colorimetric method [4], electrochemical analysis [5], and ultraviolet-visible spectrophotometry [6]. However, these methods have been limited by certain deficiencies like complicated operation, high cost, especially lack of adequate selectivity and reproducibility [7, 8]. Fortunately, the fluorescence approach as the prime alternative in analysis sensing area has attracted great interest due to their excellent advantages of operational simplicity, reliability, and cost-effectiveness [9]. Thereinto, most fluorescence methods based on QDs as nanoprobe have attracted great interest due to their rapid response [10, 11]. However, suffered from the limitation of material properties and complex surface modification during the preparing process, most of current fluorescent methods based on QDs did not show satisfactory detection selectivity and excellent detection sensitivity. Thereby, the development of QDs assays based on new fluorescent nanomaterials with high specific and desirable sensing performances has become an urgent issue for DA determination.

Xinnan Liu and Wentao Zhang contributed equally to this work.

Electronic supplementary material The online version of this article (<https://doi.org/10.1007/s00604-018-2771-0>) contains supplementary material, which is available to authorized users.

✉ Jianlong Wang
wanglong79@yahoo.com

- ¹ College of Food Science and Engineering, Northwest A&F University, Yangling 712100, Shaanxi, People's Republic of China
- ² Qinghai Key Laboratory of Qinghai-Tibet Plateau Biological Resources, Northwest Institute of Plateau Biology, Chinese Academy of Sciences, Xining 810008, Qinghai, People's Republic of China
- ³ Biological Engineering Department, Yangling Vocational & Technical College, Yangling 712100, Shaanxi, People's Republic of China

As one of transition metal dichalcogenides (TMDs) materials, natural and plentiful molybdenum disulfide (MoS_2) has received immense attention. Particularly, quantum dots of MoS_2 have been intensely studied owing to their predominant electrocatalytic and optical properties, and have shown versatile potential applications in wide areas ranging from catalysis to photodynamic therapy as well as sensors [12–14]. Especially, taking advantage of high stability, low toxicity and excellent tunable photoluminescence (PL) behaviors, MoS_2 QDs have been widely utilized in fluorescence detection. For instance, Wang et al. demonstrated the synthesis of photoluminescent MoS_2 QDs used as selective sensor for sensitive analysis of nitro explosives such as 2,4,6-trinitrophenol [15]. Gu et al. successfully prepared MoS_2 QDs via a one-step hydrothermal method as fluorescent probes to detect hyaluronidase [16]. However, the exploitation of these MoS_2 QDs has been severely hampered by synthesis methods which required sophisticated synthetic routes and long processing time. Evidently, low-cost and rapid methods for the preparation of MoS_2 QDs still remain to be proposed for practical sensing needs.

In this study, we report a convenient and ultrafast synthesis of MoS_2 QDs via an ammonium hydroxide etching method to develop a rapid and specific assay for DA detection (Scheme 1). Compared with previous synthesis methods, this novel strategy for the preparation of MoS_2 QDs within 2 min using ammonium hydroxide as etchant showed advantages of easy operation and fast fabrication. The special reaction between DA and the MoS_2 QD alkaline solution leads to the formation of organic molybdate complexes (OMCs) and dopamine–quinone, which can simultaneously quench the fluorescence of MoS_2 QDs due to the synergistic effect of ET and IFE. Thus, a novel fluorescent assay was successfully proposed for convenient one-step determination of DA with wide linear relationship and low detection limit. Furthermore, in order to evaluate the selectivity of the method, the detection was also performed through competitive reaction with interfering analytes

including ions and common substances. Finally, to verify the performance of our method in real examples, the fluorescent detection of DA in artificial urine sample were further conducted.

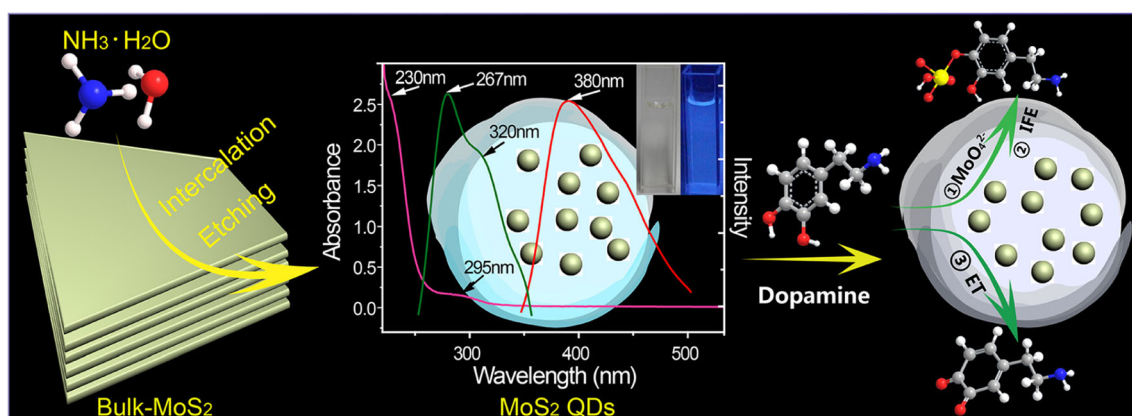
Materials and methods

Materials

Molybdenum(IV) sulfide (MoS_2) with a bulk particle size of $<2 \mu\text{m}$, cysteine and glutathione were purchased from Sigma-Aldrich (Shanghai, China, <http://www.sigmaaldrich.com/china-mainland.html>). Dopamine hydrochloride tyramine, norepinephrine, epinephrine, histamine, tryptamine hydrochloride were obtained from Aladdin chemistry Co. Ltd. (Shanghai, China, <http://www.aladdin-e.com/>). Ammonium hydroxide (25–28%), ascorbic acid, citric acid, glucose, lactic acid, urea, phenethylamine, glutamine, glutamic acid, glycine, valine, arginine, alanine, and NaNO_3 , KNO_3 , $\text{Mg}(\text{NO}_3)_2$, $\text{Ca}(\text{NO}_3)_2$, $\text{Al}(\text{NO}_3)_3$, CaCl_2 , NaHCO_3 , Na_2SO_4 , KH_2PO_4 , NH_4Cl , MgSO_4 , NaCl , K_2HPO_4 were obtained from Sinopharm Chemical Reagent Co. Ltd. (Shanghai, China, <http://www.sinoreagent.com/>). Uric acid tetracycline, ampicillin, kabamycin sulfate, streptomycin sulfate were purchased from Beijing Solarbio Science & Technology Co. Ltd. (Beijing, China, <http://www.solarbio.com/>). Doubly distilled water was used throughout the experiment. All the chemical reagents were analytical grade and used without purification.

Apparatus

Fluorescence spectra and fluorescence responses with time were measured by a LS-55 spectrometer (PerkinElmer, Britain, <http://www.perkinelmer.com.cn/>). The ultraviolet visible (UV/vis) absorption spectra were recorded on a Shimadzu UV-2550 spectrophotometer (Shimadzu, Japan,



Scheme 1 Schematic illustration of synthesis process of MoS_2 QDs and principle of the detection of DA

<http://www.shimadzu.com/>). The image of atomic force microscope (AFM) was carried out on a NanoScope V instrument with tapping mode. (Bruker, Germany, <http://www.bruker.com/>). X-ray photoelectron spectroscopy (XPS) analysis was performed on an ESCALAB 250 spectrometer (Thermo, American, <http://www.thermo.com/>). High resolution transmission electron microscopy (HRTEM) measurements were obtained with an H-600 (Hitachi, Japan, <http://www.hitachi.com/>). X-ray diffraction (XRD) measurements were performed on powder diffractometer (Bruker D8 Advanced Diffractometer System, <http://www.bruker.com/>).

Synthesis of MoS₂ QDs

MoS₂ QDs were prepared through etching bulk MoS₂ in ammonium hydroxide solution. Typically, 0.5 g of commercial MoS₂ powder was dispersed in 40 mL mixture solution, containing 55 vol.% ammonium hydroxide and 45 vol.% ethanol. The homogeneous mixture was stirred. The purified MoS₂ QDs were obtained by centrifuged at speed of 12,000 rpm for 20 min. Finally, the QD solution was stored in a refrigerator at 4 °C for further characterization and application (Note: the pH of the QD solution was measured to be ~ 9). The pure MoS₂ QDs can be obtained by dialysis with water (data not shown) and the MoS₂ QDs for the following experiment are used without further dialysis. For comparison, 0.5 g of bulk MoS₂ was dispersed in 40 mL mixture solution with different volume fraction of ammonium hydroxide (Table S1).

Detection of DA in aqueous solution

The control group was set as 2 mL water and 1 mL MoS₂ QD solution mixed in a 4 mL fluorescent cuvette at room temperature. For DA detection, mixture solution of 1 mL water and 1 mL MoS₂ QDs added into a 4 mL fluorescent cuvette at room temperature, sequentially 1 mL of DA solutions with different concentrations were added and mixed thoroughly. After incubation for 15 min at room temperature, the fluorescence spectrum of each solution was recorded accordingly to the excitation wavelength of 267 nm. The detection of DA in artificial urine samples was determined through the standard addition method by same procedure for the detection of DA in water. The preparation of the artificial urine solution was on the basis of previous reports [17, 18].

Results and discussion

Characterization of MoS₂ QDs

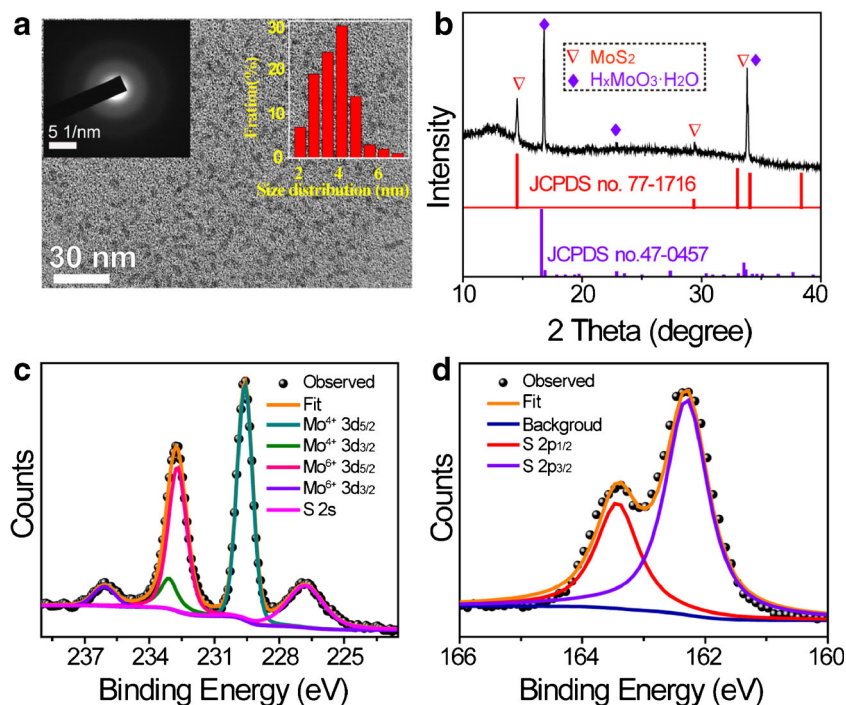
To avoid multiple steps and sophisticated equipment, the MoS₂ QDs were synthesized by a novel and rapid ammonium

hydroxide etching method. The optimal experimental condition and mechanism of the formation of the QDs were investigated in Electronic Supporting Material (Fig. S1, S2 and Table S2). The morphological structure and size distribution of prepared MoS₂ QDs were characterized by high resolution TEM (HRTEM). From Fig. 1a, it can be obtained that the QDs are well dispersed. The size distribution is presented in the inset of Fig. 1a, indicating the size of the QDs range from 2 to 7 nm with an average value ~3.7 nm. The typical selected area electron diffraction (SAED) pattern (Fig. 1a, inset) reveals that the QDs are polycrystalline, which differ from bulk MoS₂ due to the destruction and exfoliation of MoS₂ powder during ammonium hydroxide treatment [19]. The morphology and thickness of the resulting MoS₂ QDs were measured via the typical tapping atomic force microscopic (AFM) image. As shown in Fig. S3, the thickness of the resulting QDs is around 2 nm, indicating the QDs are few-layered [20]. Powder X-ray diffraction (PXRD) was further applied to explore the crystal nature of the MoS₂ quantum dots. Three obvious peaks are shown in the XRD pattern of MoS₂ QDs (Fig. 1b). The peak at 14.4 degree is the (002) plane of MoS₂ (JCPDS card no. 77–1716). The peak at 16.6 degree is assigned to HxMoO₃·H₂O (JCPDS card no. 47–0457), formed from the crystallization of molybdate ions in the QD solution during the preparation of PXRD sample. The coexistence of MoS₂ and molybdate ions in the QD solution was also verified by using X-ray photoelectron spectroscopy (XPS). The element Mo and S can be obtained in XPS spectra of MoS₂ QDs (Fig. S4). The high-resolution XPS spectrum of Mo 3d shows two characteristic peaks at 229.5 and 232.9 eV, ascribed to Mo⁴⁺ 3d_{5/2} and Mo⁴⁺ 3d_{3/2} (Fig. 1c), and those at 235.9 eV, 232.7 eV are attributed to Mo⁶⁺ 3d_{3/2}, Mo⁶⁺ 3d_{5/2} [16]. The peaks of S 2s, S 2p_{1/2} and S 2p_{3/2} are obtained at 226.7, 165.6 and 164.1 eV respectively, suggesting that sulfide ions are in –2 oxidation state [21] (Fig. 1d). The mixed-valence Mo ions exist in the MoS₂ QDs, indicating that ammonium hydroxide act as oxidant agent to convert part of Mo(IV) into Mo(VI) during the exfoliating process. Particularly, based on the previous report that Mo(VI) ions exist as the form of MoO₄²⁻ in the basic solution [22], it is reasonable that molybdate ions were generated during the preparation of MoS₂ QDs.

Optical properties of MoS₂ QDs

The UV–vis absorption spectrum and fluorescence spectrum of the QDs are shown in Fig. 2a. The absorption peak at 295 nm is shown in the UV- vis absorption spectrum, which is consistent to the previous reports [23]. Typically, for 2H-MoS₂ nanosheets, there are four characteristic peaks respectively located at 397, 454, 610 and 670 nm [19, 24]. However, these four typical peaks of 2H-MoS₂ nanosheets were disappeared in our result instead of an absorption peak

Fig. 1 **a** HRTEM image of MoS₂ QDs. The insets represent the corresponding particle size distribution histogram (top, random counting more than 100 QDs in the HRTEM image) and SAED pattern (down) of MoS₂ QDs. **b** XRD patterns of MoS₂ QDs (black line), the standard MoS₂ (JCPDS card no. 77-1716, red line) and H_xMoO₃·H₂O (JCPDS card no. 47-0457, blue line). **c-d** XPS survey spectrum of Mo 3d and S 2p



in the region of near-UV, which were attributed to the excitonic features of MoS₂ quantum dots, further verifying the collapse of bulk or nanosheet-like MoS₂ into quantum dots [23]. The fluorescence spectrum was also investigated (Fig. 2a). The fluorescence excitation spectrum recorded with the optimal luminescence showed two peaks, one at 320 nm (a shoulder peak) and one at 267 nm. The excitation peaks at 267 and 320 nm correspond to the absorption from the transitions of π to π^* and n to π^* , related to the absorption peaks at 230 and 295 nm in the absorption spectrum, respectively [25]. Correspondingly, the emission wavelength is located at 380 nm. The resultant MoS₂ QDs exhibits a transparent color under bright light and visually strong blue fluorescence under the 365 nm UV lamp (Fig. 2a, inset). The fluorescence spectra of MoS₂ QDs were then measured with different excitation

wavelengths varying from 247 to 327 nm (Fig. 2b). The fluorescent intensity of emission peak increased with the excitation wavelength from 247 to 267 nm, and the maximum emission exhibited at 380 nm excited by 267 nm light. Moreover, the fluorescent intensity of emission peak decreases with the further increasing of excitation wavelength.

Optimization of assay conditions

In order to improve the analytical performance of the QDs for the determination of DA, the following parameters were optimized: (a) Sample pH value; (b) Reaction time; (c) Amount of MoS₂ QDs; (d) Reaction temperature. Respective data and Figures are given in the Electronic Supporting Material. As shown the Fig. S5, 15 reaction time, 500 μ L QD solutions in

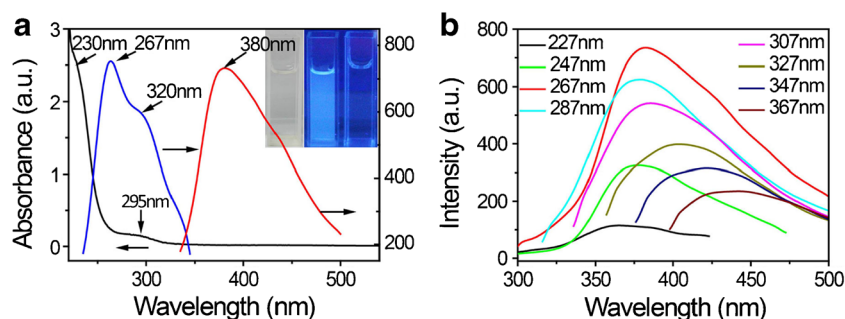


Fig. 2 **a** UV-vis absorption (black line), PL excitation (blue line), and emission (red line) spectra of the MoS₂ QDs aqueous dispersion. The insets are photographs of MoS₂ QDs in the daylight (left), under

irradiation of 365 nm light (middle) and blank control sample under irradiation of 365 nm light (right). **b** Emission spectra of MoS₂ QDs at different excitation wavelengths

pH value of 9 experiment conditions at 298 K reaction temperature were chosen the optimal experiment conditions for the subsequent assay.

Fluorescence detection of DA

The fluorescent analysis between the QD solution and different concentrations of DA were investigated. It is obvious that the fluorescence intensity at 380 nm with excitation at 267 nm was monotonically decreased with the increase of the DA concentration (Fig. 3a and b). The calibration curve was then constructed by plotting quenching intensity ($F_0 - F$), and a good linear equation of $(F_0 - F) = 1.1565 \times + 28.7040$ was obtained in the concentrations range of DA from 0.1 to 2.5 μM ($R^2 = 0.9972$) (Fig. 3c). The limit of detection (LOD) for DA was estimated to be 0.01 μM according to the $3S/N$ principle, where S is the standard deviation of the blank signals and N is the slope of the calibration curve [26]. Moreover, the fluorescence intensity also linearly decreases with a response of $(F_0 - F) = 2.4892 \times + 67.2303$ ($S/N = 3$, $R^2 = 0.9984$) with the concentration of DA ranging from 2.5 to 100 μM (Fig. 3d). Compared with other reported methods (Table S3), our unique MoS_2 QDs as new fluorescence sensor display comparable performance for the detection of DA.

Selectivity for DA detection

To test the selectivity of the QDs for DA analysis, various representative similar substances, including organic compounds, biogenic amines, amino acids, antibiotics and metal ions were examined at the same conditions. As shown in Fig. 3e, only DA can obviously quench the fluorescence of the QDs, the interferences show negligible quenching effect except norepinephrine, epinephrine, and tetracycline, which present certain interference within the tolerable scope. To further verify the specificity of the method to detect DA, the fluorescence intensities of the QD solution containing DA coexistent with interferences were measured (Fig. 3f). The quenching ratio show weak difference with that of quenched by DA alone except the norepinephrine, epinephrine and tetracycline. The reason is owing to that the norepinephrine and epinephrine have the similar structures with DA, they may be influence the analytical ability of the QDs. The absorbance peak of tetracycline has a small overlap of the emission spectrum which may cause inner filter effect to influence the fluorescence of the QDs. However, in practical, the levels of these are substantially lower than that of the DA in the biological fluids such as cerebrospinal fluid [9, 27]. Thus, these interferences have applicable influence on the detection of DA in practical assay, indicating the selectivity of this assay.

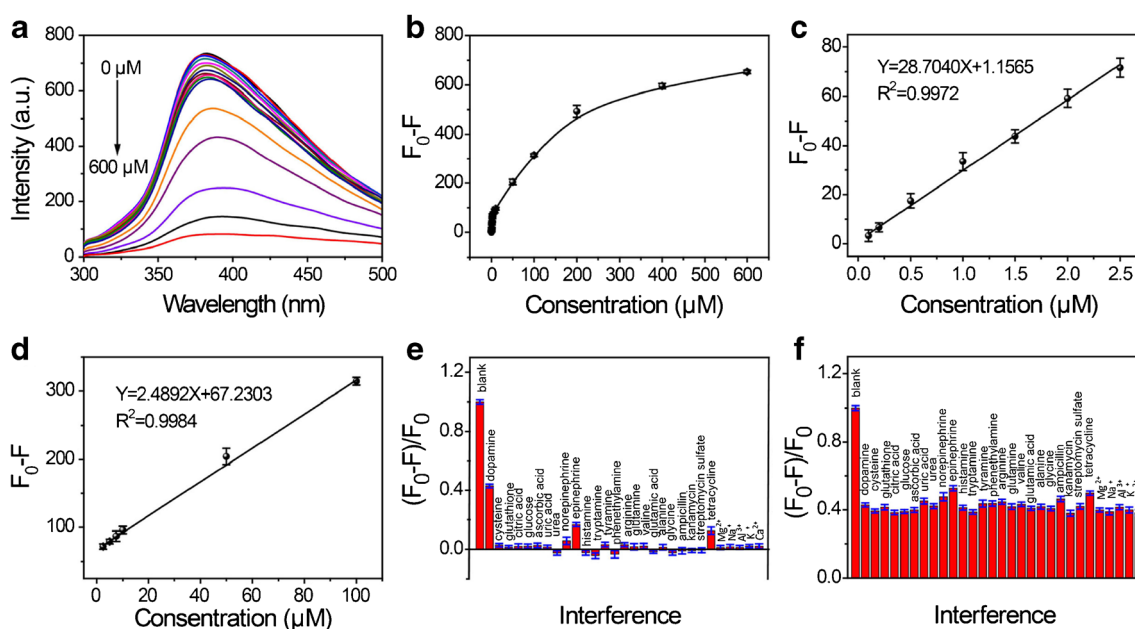
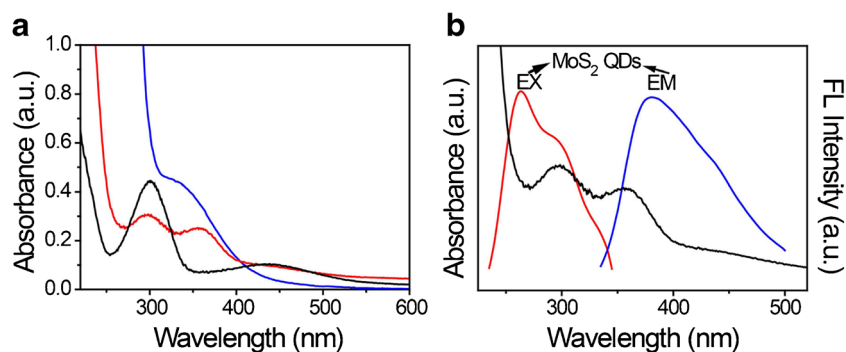


Fig. 3 **a** The fluorescence emission spectra of MoS_2 QDs in the presence of DA with different concentrations. **b** The relationship between the concentration of DA and quenching fluorescence intensity. ($\lambda_{\text{em}} = 380 \text{ nm}$) **c** Calibration plot of the $(F_0 - F)$ to various concentrations of DA ranging from 0.1–2.5 μM . ($\lambda_{\text{em}} = 380 \text{ nm}$) **d** Calibration plot of the

$(F_0 - F)$ to different concentrations of DA ranging from 2.5 μM to 100 μM . ($\lambda_{\text{em}} = 380 \text{ nm}$) **e** The fluorescence intensities of MoS_2 QDs with DA, interferences and no interference. **f** The fluorescence response of MoS_2 QDs with DA, mixture of DA and interferences, and blank (DA and interference substances with additional concentration of 100 μM)

Fig. 4 **a** UV–vis absorption spectra of ammonium molybdate with dopamine in basic solution (blue line), dopamine in basic solution (black line) and mixture of MoS₂ QDs with dopamine (red). **b** The excitation spectrum (red), emission spectrum of MoS₂ QDs (blue), and UV-vis absorption spectra of MoS₂ QDs treated with DA (black)



The possible mechanism of the DA detection

To investigate the quenching type of the quenching process, we discussed the Stern–Volmer plot following the equation [28].

$$F_0/F = 1 + K_{sv}[Q]$$

where the F_0 and F are the fluorescence intensity at 380 nm in absence and presence of DA, K_{sv} is the Stern–Volmer quenching constant, $[Q]$ is the concentration of DA. As depicted in the Fig. S6A, there is a good linear relationship between the F_0/F and different concentrations which indicates that only one quenching type exists in the quenching process [29], and the value of K_{sv} is calculated to be $4.30 \times 10^4 \text{ L mol}^{-1}$. In order to justify the type of the quenching mechanism, the Stern–Volmer quenching constant in different temperatures were measured (Fig. S6B). As shown in Table S4, the values of fluorescence quenching constants were increasing with the increase of the temperature, demonstrating that the dynamic quenching dominates the quenching system [30].

In order to further investigate the mechanism of this proposed method, the absorption peaks of the possible existent products of system were investigated. As shown in Fig. 4a, the resultants of the QD solution with DA show three obvious peaks at about 300 nm, 360 nm, and 450 nm, respectively. In order to explicate the origins of these three peaks, we further test the absorption peak of ammonium molybdate with dopamine in basic solution, and the absorption peak change of dopamine at basic pH same as our system. Compared with the results shown in Fig. 4a, the peak at 300 nm of our quenching system is assigned to DA with a slight shift. The peak around at 450 nm belongs to dopamine–quinone, which corresponds to the previous reports [31]. It has been reported that catechol and related compounds (at least two ortho hydroxyl groups) yield yellow to orange-brown complexes with molybdate ions, forming organic molybdate complexes (OMCs) [32]. Therefore, DA with ortho hydroxyl groups can react with molybdate ions forming OMCs with a peak near 345 nm [33]. Once in the PL quenching system, a red shift from 345 nm to

360 nm is observed for organic molybdate complexes, which might be attributed to the rather complex chemical condition of quenching system. Subsequently, we investigated the overlap between the excitation, emission spectrum of MoS₂ QDs and absorption spectra of the products of MoS₂ QDs reacting with DA. As exhibited in Fig. 4b, the absorption band of DA react with the MoS₂ QDs show overlap over the excitation and emission spectrum of MoS₂ QDs. This phenomenon can lead to the inner filter effect (IFE) due to the phenomena that absorption band of the absorber presents an overlap with the excitation and/or emission of the fluorescent substance [34]. On the other hand, it is well known that DA can be easily oxidized to dopamine–quinone by ambient oxygen at the basic solution. And the generating dopamine–quinone acts as electron acceptor, which can partially quench the fluorescence of QDs during the electron transfer (ET) process [35]. Therefore, based on the excellent synergistic effect of IFE and ET of our unique quenching system, MoS₂ QDs should possess highly efficient and selectivity for the detection of DA.

Application in artificial urine samples

To illustrate the analytical applicability of our method, we then determined DA in artificial urine samples by standard addition method. Firstly, we certified the selectivity of the method at the detectable LOD. Compared with blank sample, no obvious change of fluorescence quenching ratio was observed when DA coexisting with interferences. Thus the

Table 1 The results of detection of DA in artificial urine

Sample	Spiked (μM)	Found (μM)	Recovery (%)	^a RSD (%)
1	0.20	0.20	100.8	4.54
2	0.50	0.49	97.6	1.14
3	1.00	1.02	102.2	3.04

^a The relative standard deviations (RSD) were measured from three values for every sample

QDs showed selective detection results at detectable LOD in the practical assay (Fig. S7). As shown in Fig. S8, the 200-fold dilution was taken as the artificial urine samples. Thus, DA was added into the practical samples with final three levels concentration of 0.2, 0.5 and 1.0 μM , respectively. As depicted in Table 1, the recovery is ranged from 97.6% to 102.2%, and the relative standard deviation (RSD) is ranged from 1.14% to 4.54%, demonstrating that the QD solution can be acceptably applied in analysis for DA in real samples.

Conclusions

In summary, a novel and highly selective fluorometric assay for determination of DA has been successfully developed. The probe based on unique MoS_2 QDs was rapidly synthesized via ammonium hydroxide etching method in 2 min. This method was applied into the direct determination of DA in few minutes without addition of other triggers, and results showed good linear relationship, high sensitivity and excellent specificity. Moreover, for the analysis of DA in artificial urine sample, this novel probe still presented well accuracy and satisfactory reproducibility. However, the further work can be aiming to provide a highly specific probe for DA analysis avoiding the influence resulted from biomaterial under the UV excitation. Therefore, this contribution provides a good potential alternative in detection to DA analysis for clinical diagnosis.

Acknowledgments This research was financed by the National Natural Science Foundation of China (21675127), the Fundamental Research Funds for the Northwest A&F University of China (2014YB093, 2452015257) and the Development Project of Qinghai Key Laboratory (2017-ZJ-Y10).

Compliance with ethical standards The author(s) declare that they have no competing interests.

References

- Li B-R, Hsieh Y-J, Chen Y-X, Chung Y-T, Pan C-Y, Chen Y-T (2013) An ultrasensitive nanowire-transistor biosensor for detecting dopamine release from living PC12 cells under hypoxic stimulation. *J Am Chem Soc* 135(43):16034–16037
- Yildirim A, Bayindir M (2014) Turn-on fluorescent dopamine sensing based on in situ formation of visible light emitting Polydopamine nanoparticles. *Anal Chem* 86(11):5508–5512
- De Benedetto GE, Fico D, Pennetta A, Malitesta C, Nicolardi G, Lofrumento DD, De Nuccio F, La Pesa V (2014) A rapid and simple method for the determination of 3,4-dihydroxyphenylacetic acid, norepinephrine, dopamine, and serotonin in mouse brain homogenate by HPLC with fluorimetric detection. *J Pharm Biomed Anal* 98:266–270
- Wen D, Liu W, Herrmann A-K, Haubold D, Holzschuh M, Simon F, Eychmueller A (2016) Simple and sensitive colorimetric detection of dopamine based on assembly of cyclodextrin-modified Au nanoparticles. *Small* 12(18):2439–2442
- Anithaa AC, Lavanya N, Asokan K, Sekar C (2015) WO_3 nanoparticles based direct electrochemical dopamine sensor in the presence of ascorbic acid. *Electrochim Acta* 167:294–302
- Xu Q, Yoon J (2011) Visual detection of dopamine and monitoring tyrosinase activity using a pyrocatechol violet- Sn^{4+} complex. *Chem Commun* 47(46):12497–12499
- Diaz-Diestra D, Thapa B, Beltran-Huarac J, Weiner BR, Morell G (2017) L-cysteine capped ZnS:Mn quantum dots for room-temperature detection of dopamine with high sensitivity and selectivity. *Biosens Bioelectron* 87:693–700
- Yang Q, Wang Y, Wang J, Liu F, Hu N, Pei H, Yang W, Li Z, Suo Y, Wang J (2018) High effective adsorption/removal of illegal food dyes from contaminated aqueous solution by Zr-MOFs (UiO-67). *Food Chem* 254:241–248
- Wang B, M-m C, H-q Z, Wen W, Zhang X-h, S-f W (2017) A simple and sensitive fluorometric dopamine assay based on silica-coated CdTe quantum dots. *Microchim Acta* 184(9):3189–3196
- Zhou X, Ma P, Wang A, Yu C, Qian T, Wu S, Shen J (2015) Dopamine fluorescent sensors based on polypyrrole/graphene quantum dots core/shell hybrids. *Biosens Bioelectron* 64:404–410
- Rasheed PA, Lee J-S (2017) Recent advances in optical detection of dopamine using nanomaterials. *Microchim Acta* 184(5):1239–1266
- Dong H, Tang S, Hao Y, Yu H, Dai W, Zhao G, Cao Y, Lu H, Zhang X, Ju H (2016) Fluorescent MoS_2 quantum dots: ultrasonic preparation, up-conversion and down-conversion bioimaging, and photodynamic therapy. *ACS Appl Mater Interfaces* 8(5):3107–3114
- Zhang W, Shi S, Wang Y, Yu S, Zhu W, Zhang X, Zhang D, Yang B, Wang X, Wang J (2016) Versatile molybdenum disulfide based antibacterial composites for in vitro enhanced sterilization and in vivo focal infection therapy. *Nano* 8(22):11642–11648
- Cao H, Wang H, Huang Y, Sun Y, Shi S, Tang M (2017) Quantification of gold(III) in solution and with a test stripe via the quenching of the fluorescence of molybdenum disulfide quantum dots. *Microchim Acta* 184(1):91–100
- Wang Y, Ni Y (2014) Molybdenum disulfide quantum dots as a photoluminescence sensing platform for 2,4,6-Trinitrophenol detection. *Anal Chem* 86(15):7463–7470
- Gu W, Yan Y, Zhang C, Ding C, Xian Y (2016) One-step synthesis of water-soluble MoS_2 quantum dots via a hydrothermal method as a fluorescent probe for hyaluronidase detection. *ACS Appl Mater Interfaces* 8(18):11272–11279
- Mohammadi S, Maeki M, Mohammadi RM, Ishida A, Tani H, Tokeshi M (2015) An instrument-free, screen-printed paper microfluidic device that enables bio and chemical sensing. *Analyst* 140(19):6493–6499
- Wang J, Yang Q, Zhang L, Liu M, Hu N, Zhang W, Zhu W, Wang R, Suo Y, Wang J (2018) A hybrid monolithic column based on layered double hydroxide-alginate hydrogel for selective solid phase extraction of lead ions in food and water samples. *Food Chem* 257:155–162
- Xu S, Li D, Wu P (2015) One-pot, facile, and versatile synthesis of monolayer MoS_2/WS_2 quantum dots as Bioimaging probes and efficient electrocatalysts for hydrogen evolution reaction. *Adv Funct Mater* 25(7):1127–1136
- Wang Y, Ou JZ, Balendhran S, Chrimes AF, Mortazavi M, Yao DD, Field MR, Latham K, Bansal V, Friend JR, Zhuykov S, Medhekar NV, Strano MS, Kalantar-zadeh K (2013) Electrochemical control

- of photoluminescence in two-dimensional MoS₂ nanoflakes. *ACS Nano* 7(11):10083–10093
21. Kibsgaard J, Chen Z, Reinecke BN, Jaramillo TF (2012) Engineering the surface structure of MoS₂ to preferentially expose active edge sites for electrocatalysis. *Nat Mater* 11(11):963–969
 22. Yin Z, Zhang X, Cai Y, Chen J, Wong JI, Tay Y-Y, Chai J, Wu J, Zeng Z, Zheng B, Yang HY, Zhang H (2014) Preparation of MoS₂-MoO₃ hybrid nanomaterials for light-emitting diodes. *Angew Chem Int Ed* 53(46):12560–12565
 23. Chikan V, Kelley DF (2002) Size-dependent spectroscopy of MoS₂ nanoclusters. *J Phys Chem B* 106(15):3794–3804
 24. Zhang W, Wang Y, Zhang D, Yu S, Zhu W, Wang J, Zheng F, Wang S, Wang J (2015) A one-step approach to the large-scale synthesis of functionalized MoS₂ nanosheets by ionic liquid assisted grinding. *Nano* 7(22):10210–10217
 25. Li BL, Chen LX, Zou HL, Lei JL, Luo HQ, Li NB (2014) Electrochemically induced Fenton reaction of few-layer MoS₂ nanosheets: preparation of luminescent quantum dots via a transition of nanoporous morphology. *Nano* 6(16):9831–9838
 26. Chen M, Zheng Y, Gao J, Li C, Yu C, Wang Q (2017) Fluorometric determination of dopamine by using a terbium (III) inorganic-organic network. *Microchim Acta* 184(7):2275–2280
 27. Devi JSA, Anulekshmi AH, Salini S, Aparna RS, George S (2017) Boronic acid functionalized nitrogen doped carbon dots for fluorescent turn-on detection of dopamine. *Microchim Acta* 184(10):4081–4090
 28. Wang F, Hao Q, Zhang Y, Xu Y, Lei W (2016) Fluorescence quenchometric method for determination of ferric ion using boron-doped carbon dots. *Microchim Acta* 183(1):273–279
 29. Xu H, Yang X, Li G, Zhao C, Liao X (2015) Green synthesis of fluorescent carbon dots for selective detection of Tartrazine in food samples. *J Agric Food Chem* 63(30):6707–6714
 30. Sahoo D, Mandal A, Mitra T, Chakraborty K, Bardhan M, Dasgupta AK (2018) Nanosensing of pesticides by zinc oxide quantum dot: an optical and electrochemical approach for the detection of pesticides in water. *J Agric Food Chem* 66(2):414–423
 31. Guo X, Wu F, Ni Y, Kokot S (2016) Synthesizing a nano-composite of BSA-capped Au nanoclusters/graphitic carbon nitride nanosheets as a new fluorescent probe for dopamine detection. *Anal Chim Acta* 942:112–120
 32. Yue X, Liu L, Li Z, Yang Q, Zhu W, Zhang W, Wang J (2018) Highly specific and sensitive determination of propyl gallate in food by a novel fluorescence sensor. *Food Chem* 256:45–52
 33. Liao X, Lang H, Xu W, Shen Y (2003) Determination of polyphenols in tea by ammonium molybdate spectrophotometry. *Chin J Anal Lab* 05:70–72 (in Chinese)
 34. Tang Z, Lin Z, Li G, Hu Y (2017) Amino nitrogen quantum dots-based nanoprobe for fluorescence detection and imaging of cysteine in biological samples. *Anal Chem* 89(7):4238–4245
 35. Zhao J, Zhao L, Lan C, Zhao S (2016) Graphene quantum dots as effective probes for label-free fluorescence detection of dopamine. *Sensors Actuators B Chem* 223:246–251